1-5-2005

Speckle noise modeling and reduction of SAR Images based Markov random fields

Ousseini Lankoande

Majeed M. Hayat

Bal Santhanam

DEPARTMENT OF ELECTRICAL AND COMPUTER ENGINEERING

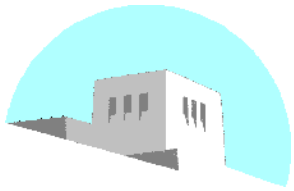

SCHOOL OF ENGINEERING

UNIVERSITY OF NEW MEXICO

Speckle noise modeling and reduction of SAR images based on Markov random fields

Ousseini Lankoande
Department of Electrical and Computer Engineering
The University of New Mexico
Albuquerque, NM 87131
e-mail: lankoande@ece.unm.edu

Majeed M. Hayat
Department of Electrical and Computer Engineering
The University of New Mexico Albuquerque, NM 87131
Phone: (505) 277-0297, Fax: (505) 277-1439
e-mail: hayat@ece.unm.edu

Balu Santhanam
Department of Electrical and Computer Engineering
The University of New Mexico Albuquerque, NM 87131
Phone: (505) 277-1611, Fax: (505) 277-1439
e-mail: bsanthan@ece.unm.edu

UNM Technical Report: EECE-TR-2004-26

Report Date: January 5, 2005

Abstract

One of the major factors plaguing the performance of synthetic aperture radar (SAR) imagery is the signal-dependent, speckle noise. Grainy in appearance, it is due to the phase fluctuations of the electromagnetic returned signals. Since the inherent spatial-correlation characteristics of speckle in SAR images are not embedded in the multiplicative models for speckle noise, a new mathematical framework for modeling speckled imagery is introduced. It is based on embedding the spatial correlation properties of speckled imagery, obtained from statistical optics, into a Markov-random-field (MRF) framework. The model is then used to perform speckle-noise reduction through the utilization of a global energy-minimization algorithm, which consists of simulated annealing in conjunction with the Metropolis sampler algorithm. A comparative study using both simulations and real SAR images indicates that the proposed approach performs better compared to filtering techniques such as the Gamma Map, the modified-Lee and the enhanced-Frost algorithms. This success is attributable to the ability of the proposed model to capture the physical spatial statistics of speckle within the confines of a MRF framework.

Keywords

speckle modeling, speckle reduction, synthetic aperture radar, SAR imaging, Markov random fields.

1 Introduction

Synthetic aperture radar (SAR) is a type of imaging system that uses coherent radiation to create images. The major advantage of SAR over non-radar imaging systems is that it does not rely on an external source. As an active system, SAR emits its own radiations and remains effective independently of weather or daylight conditions [8]. Unfortunately, this autonomy comes with a higher susceptibility to speckle noise.

A SAR system coherently records the amplitude and the phase echoed from a target. Since each resolution cell of the system contains several scatterers, and since the phases of the returned signals from these scatterers are randomly distributed, the inherent coherent processing involved results in interference noise like patterns also called speckle. A large variety of speckle-reduction techniques have been proposed in the literature. Among them are the Lee filter and its derivatives [12, 5], the geometric filter [15], the Kuan filter [11], the Frost filter and its derivatives [5, 9], the Gamma MAP filter [5], the wavelet approach [2, 6] and the approaches based on *Markov-random-fields* (MRFs) [17, 7]. These approaches assume a multiplicative model for the speckled image intensity hence each observed image pixel is the product of the noise-free image pixel with the noise [16]. The capability of MRFs to model spatially correlated and signal-dependent phenomena makes them an excellent choice for modeling speckled images. However, exiting MRF-based methods for speckle are not derived from the physical statistical properties of speckle.

In this report, the multiplicative model is not assumed; instead, we assume that the observed speckled intensity image is one of the configurations of our MRF model whose high energy has to be reduced through de-noising. We derive a novel MRF model for speckled imagery based on the spatial-correlation properties of speckle, which are obtained from the literature on statistical optics [4]. More precisely, Goodman [4] has derived the joint conditional probability density function (cpdf) of the speckled intensity of any two points. In this work, we have incorporated this cpdf into a MRF model, which makes the resulting MRF model in tune with the physical attributes of speckled imagery. With the availability of this MRF model, the noise reduction of SAR images is undertaken using a global energy-minimization algorithm based on using simulated annealing (SA) [10] in conjunction with the Metropolis sampler [13].

2 First order MRF model

A MRF consists of an undirected graph $G = (V, E)$ that has undirected edges drawn as lines. The set V of vertices of the graph is $\{I_k, I_{k_1}, I_{k_2}, I_{k_3}, I_{k_4}\}$ and E is the set of edges. Two type of cliques can be defined for the graph in Figure 1a. The single-clique: $C_1 = \Big\{(x_k, y_k), k \in S\Big\}$, and the pair-clique, $C_2 = \Big\{ \{(x_k, y_k), (x_{k_1}, y_{k_1})\}, \{(x_k, y_k), (x_{k_2}, y_{k_2})\}, \{(x_k, y_k), (x_{k_3}, y_{k_3})\}, \{(x_k, y_k), (x_{k_4}, y_{k_4})\} k \in S, k_i \in S, i = 1, \cdots, 4 \Big\}$, where S is the set of indexes of the image. The *conditional probability density* (cpd) function of the intensity I_{k_j} at point k_j given the value of the intensity I_{k_i} at point k_i is drawn from statistical optics theory and provided by Goodman in [4]. Here, the global mean, $\langle I \rangle$, has been substituted by $(i_t)_{k_j}$, which is defined as the true intensity image at point k_j. The realization of the random variable I_{k_j} at point k_j is denoted by i_{k_j}. More precisely,

$$p_{I_{k_j}|I_{k_i}}(i_{k_j}|i_{k_i}) = \frac{\exp\Big(-\frac{|\mu(r_{k_i k_j})|^2 i_{k_i} + i_{k_j}}{(i_t)_{k_j}(1-|\mu(r_{k_i k_j})|^2)}\Big)}{(i_t)_{k_j}(1-|\mu(r_{k_i k_j})|^2)} I_0\Big(\frac{2(i_{k_i} i_{k_j})^{1/2}|\mu(r_{k_i k_j})|}{(i_t)_{k_j}(1-|\mu(r_{k_i k_j})|^2)}\Big), \tag{1}$$

where $I_0(\cdot)$ is a modified Bessel function of the first kind and zero order, and $|\mu(r_{k_i k_j})|$ and $r_{k_i k_j}$ are, respectively, the coherence factor and the Euclidian distance between the points k_i and k_j. For simplicity, we assume that the coherence factor has the following form (other more complex forms can also be considered):

$$|\mu(r_{k_i k_j})| = \begin{cases} |\alpha_{r_{k_i k_j}}| \in [0,1) & r_{k_i k_j} \leq 1 \\ 0 & \text{otherwise.} \end{cases} \tag{2}$$

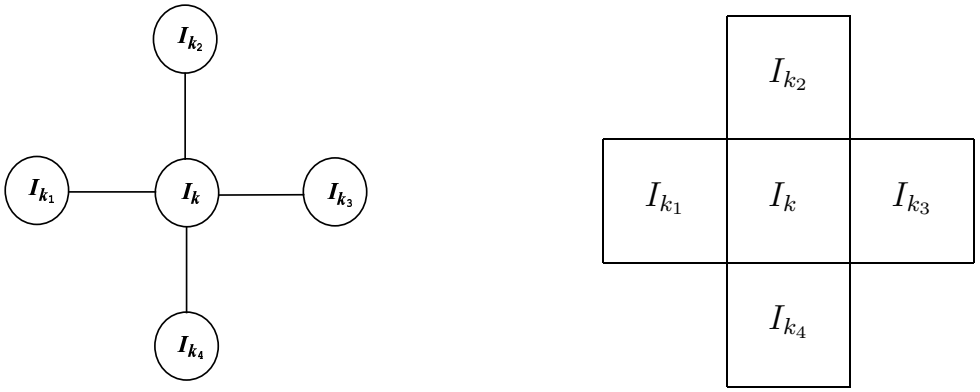

(a) (b)

Figure 1: (a) Graph form of the first-order neighborhood. (b) Lattice form of the first-order neighborhood.

If $r_{k_i k_j} > 1$, then the cpdf in (1) becomes independent of i_{k_i} and $p_{I_{k_j}|I_{k_i}}(i_{k_j}|i_{k_i}) = p_{I_{k_j}}(i_{k_j}) = \exp\big(-\frac{i_{k_j}}{(i_t)_{k_j}}\big)/(i_t)_{k_j}$. In addition, the correlation in (2) is assumed to be limited to one unit from the center pixel. This condition can still be met with larger correlation (more than one unit correlation) by preprocessing the data. Indeed, in the case of an image having a larger correlation we will apply one of the interpolation methods in order for the correlation to fit the above definition of the coherence factor [7]. The Euclidian distance between the pair of pixels (i_{k_1}, i_{k_2}), (i_{k_2}, i_{k_3}), (i_{k_3}, i_{k_4}), (i_{k_4}, i_{k_1}),(i_{k_2}, i_{k_4}) and (i_{k_1}, i_{k_3}), is either $\sqrt{2}$ or 2; in both cases, the distance is greater than 1 unit. Using the coherence factor defined in (2), we can conclude that these pairs of pixels are conditionally independent given the center pixel i_k. Then cpdf of the intensity of the center pixel, i_k, given the four neighbors i_{k_1}, i_{k_2}, i_{k_3} and i_{k_4} takes the following form:

$$p_{I_k|I_{k_{1\cdots 4}}}(i_k|i_{k_{1\cdots 4}}) = \frac{p_{I_k|I_{k_1}}(i_k|i_{k_1})\, p_{I_k|I_{k_2}}(i_k|i_{k_2})\, p_{I_k|I_{k_3}}(i_k|i_{k_3})\, p_{I_k|I_{k_4}}(i_k|i_{k_4})}{\Big(p_{I_k}(i_k)\Big)^3}. \tag{3}$$

Recall that each term in (3) is precisely known using (1); therefore, after substitution we obtain

$$p_{I_k|I_{k_{1\cdots 4}}}(i_k|i_{k_{1\cdots 4}}) = \exp\Bigg\{ \sum_{j=1}^{4} -\ln[B(i_k,i_{k_j})] - \frac{A(i_k,i_{k_j})}{B(i_k,i_{k_j})} + \ln\Big\{ I_0\big[\frac{C(i_k,i_{k_j})}{B(i_k,i_{k_j})}\big]\Big\} - 3\ln[p_{I_k}(i_k)]\Bigg\} \tag{4}$$

where $A(i_k,i_{k_j}) = |\alpha_{r_{kk_j}}|^2 i_{k_j} + i_k$, $B(i_k,i_{k_j}) = (i_t)_k(1-|\alpha_{r_{kk_j}}|^2)$, and $C(i_k,i_{k_j}) = 2(i_k i_{k_j})^{1/2}|\alpha_{r_{kk_j}}|$.
The cpdf obtained in (4) has the form

$$\begin{aligned} p_{I_k|I_{k_{1\cdots 4}}}(i_k|i_{k_{1\cdots 4}}) &= \exp\big[-U(i_k,i_{k_{1\cdots 4}})\big], \text{ where} \\ U(i_k,i_{k_{1\cdots 4}}) &= V_{C_1}(i_k) + V_{C_2}(i_k,i_{k_{1\cdots 4}}) \text{ and} \\ V_{C_1}(i_k) = 3\ln\big[p_{I_k}(i_k)\big];\; V_{C_2}(i_k,i_{k_{1\cdots 4}}) &= \sum_{j=1}^{4}\Big\{\frac{A(i_k,i_{k_j})}{B(i_k,i_{k_j})} - \ln\Big[I_0\big[\frac{C(i_k,i_{k_j})}{B(i_k,i_{k_j})}\big]\Big] + \ln\big[B(i_k,i_{k_j})\big]\Big\}. \end{aligned} \tag{5}$$

From the Hammersley-Clifford theorem [3], the energy function is identified to be $U(i_k,i_{k_{1\cdots 4}})$. The terms $V_{C_1}(i_k)$ and $V_{C_2}(i_k,i_{k_{1\cdots 4}})$ are, respectively, the single-clique and the pair-clique potential functions. The above energy function will be utilized in the speckle reduction process.

3 Simulation and Experimental Results

3.1 Image quality assessment parameters

The assessment of the speckle reduction quality will be based on four metrics. The first metric is the *mean square error* (MSE) between the noise-free and the denoised images having each K pixels; it is defined as follows

$$MSE = K^{-1}\sum_{i=1}^{K}(I_i - \widehat{I}_i)^2.$$

The second metric is the so-called β parameter used in [6], which assesses the quality of the edge preservation. It is defined by

$$\beta = \frac{\Gamma(\mathrm{I_H} - \overline{\mathrm{I_H}}, \widehat{\mathrm{I_H}} - \overline{\widehat{\mathrm{I_H}}})}{\sqrt{\Gamma(\mathrm{I_H} - \overline{\mathrm{I_H}}, \mathrm{I_H} - \overline{\mathrm{I_H}})\Gamma(\widehat{\mathrm{I_H}} - \overline{\widehat{\mathrm{I_H}}}, \widehat{\mathrm{I_H}} - \overline{\widehat{\mathrm{I_H}}})}}.$$

with $\Gamma(I_1, I_2) = \sum_{i=1}^{K} I_{1_i} I_{2_i}$. The best preservation coefficient is 1. The quantities I_H and $\widehat{I_H}$ are the highpass filtered versions of I and $\widehat{I}$, respectively (using the Laplacian operator), and I and $\widehat{I}$ represent the original (or noise free) and the noisy (or despeckle) intensity image, respectively. The third metric, which is the *signal-to-noise ratio* (SNR) in db is defined by

$$\mathrm{SNR} = 10\log_{10}\left(\frac{\sum_{\mathrm{j=1}}^{\mathrm{K}} \mathrm{I_i}^2}{\sum_{\mathrm{j=1}}^{\mathrm{K}} \left(\mathrm{I_i} - \widehat{\mathrm{I}}_\mathrm{i}\right)^2}\right).$$

The forth and final metric is the *effective number of looks* (ENL); it is often used to estimate the speckle noise level in a SAR image [7]. The higher the parameter the lower the speckle noise in the area will be. The ENL is used to assess the reduction performance not only on simulated but also on real speckled images. It is obtained by using the mean and variance intensity over a uniform area as follows

$$\mathrm{ENL} = \frac{(\mathrm{mean}^2)_{\mathrm{UniformArea}}}{(\mathrm{variance})_{\mathrm{UniformArea}}}.$$

3.2 Proposed speckle reduction approach using the simulated annealing (SA) with the Metropolis sampler algorithm

In this section we describe our proposed speckle reduction approach, which combined the SA and the *Metropolis sampler* (MS). In what follows, a narrative description of the proposed approach for purpose of clarity is first given and it is followed by a detailed mathematical description of the algorithm.

The de-noising process essentially works as follows: For each pixel of the image, an initial test, termed the uniformity test, is performed to determine if the pixel is a candidate for de-noising. This test is done by calculating the intensity variability within a window W_k (of size 3×3 in this report) centered about the pixel in question (the details are given below). The test also looks for the presence of lines, which may results in high intensity variability that is not attributed to the noise. Low variability in intensity or high variability in the presence of lines (within a W_k neighborhood of the pixel) are indicative of relative homogeneity, which implies, in turn, the "absence" of noise. In such a case, the pixel's intensity is left unaltered and we move to the next pixel. On the other hand, if the intensity variability is high and no lines are detected, the pixel will be subjected to the *simulated annealing-Metropolis sampler* (SA-MS) procedure for de-noising. The SA-MS works by updating the pixel's intensity according to the energy function (which is obtained from the MRF model) whose temperature T is allowed to gradually decrease [7, 10]. In particular, an energy difference, ΔU, is calculated between the energies before and after the pixel's intensity is updated with a candidate intensity. This energy difference is then used to accept or reject the pixel's candidate intensity based on a rejection/acceptance sampling scheme. Once the

update step is completed for a pixel, the next pixel is considered and handled similarly and the entire procedure is repeated until all pixels in the image are exhausted. Note that the uniformity test described above also serves as a stopping criterion and mechanism for the SA-MS algorithm.

The detailed mathematical description of the algorithm is now described as follows:
Step 1: Initialization stage:

- Set the initial temperature T_0
- Set the coherence factor $\alpha_{r_{kk_j}}$
- Set the parameter λ, which controls the cooling scheme
- Set the parameter δ, which is the threshold for line or noise detection
- Set the parameter γ, which is the threshold number of pixels within the window W_k of size 3×3 centered in i_k whose variations are below δ

Step 2: Perform the uniformity test
Consider the kth pixel with intensity i_k
Extract W_k and compute the variation of intensities about the center pixel i_k as follows: $\Delta W_{kk_j} = |i_k - W_{k_j}|,\ j = 1, \cdots, 8$. Next, evaluate the following (see Figure 2):

1. $N_k = \sum_{j=1}^{8} (\Delta W_{kk_j} < \delta)$. This is the number of pixels within W_k whose intensities are similar (i.e., less than δ apart) to the intensity of the center pixel.
2. Perform the uniform-neighborhood test: $U = (N_k \geq \gamma)$
3. Horizontal line test: $H = \{(\Delta W_{kk_1} < \delta) \& (\Delta W_{kk_5} < \delta)\}$
4. Vertical line test: $V = \{(\Delta W_{kk_3} < \delta) \& (\Delta W_{kk_7} < \delta)\}$
5. 1st oblique line test: $O_1 = \{(\Delta W_{kk_2} < \delta) \& (\Delta W_{kk_6} < \delta)\}$
6. 2nd oblique line test: $O_2 = \{(\Delta W_{kk_4} < \delta) \& (\Delta W_{kk_8} < \delta)\}$

W_{k_2}	W_{k_3}	W_{k_4}
W_{k_1}	W_{k_0}	W_{k_5}
W_{k_8}	W_{k_7}	W_{k_6}

(a)

ΔW_{kk_2}	ΔW_{kk_3}	ΔW_{kk_4}
ΔW_{kk_1}	0	ΔW_{kk_5}
ΔW_{kk_8}	ΔW_{kk_7}	ΔW_{kk_6}

(b)

Figure 2: (a) The window W_k centered on the kth pixel (b) Corresponding window after subtraction of i_k

Line/noise detection and the SA-MS process:
Test: Is (U or H or V or O_1 or O_2) true ?
If yes, the intensity i_k is unchanged.
If no a large variability has been detected and i_k is possibly noisy. Therefore proceeds to update the intensity:
Step 3: Perform intensity update

1. Generate $i_{k_{\text{new}}} \in L \backslash \{i_k\}$ at random with $L \backslash \{i_k\}$ being the set of grey levels except i_k

2. Update the temperature with $T_k = \lambda \times T_{k-1}$
3. Compute $p = \min\{1, e^{-\Delta U/T_k}\}$, where $\Delta U = U(i_{k_{\text{new}}}, i_{k_{1\cdots 4}}) - U(i_k, i_{k_{1\cdots 4}})$
4. Acceptance/Rejection step:
   (a) Generate a uniformly-distributed r.v. $R \in [0,1]$
   (b) If $R < p$ then accept $i_{k_{\text{new}}}$, i.e., $i_k \leftarrow i_{k_{\text{new}}}$
   (c) If $R \geq p$ then reject $i_{k_{\text{new}}}$, i.e., i_k is unchanged

Step 4: Repeat steps 2 and 3 for the next pixel
Increment k and go to Step-2 until $k = M \times N$, the $M \times N$ being the size of the image.
Step 5: Repeat steps 2-4 until the uniformity test is positive for almost every pixel.

Steps 2-4 constitute one iteration of the SA-MS scheme. The test at the end of Step 2 constitutes a reliable criterion (based on our experience) to assess when to end the update of the intensities and hence gives us a stopping criterion. Indeed, if the test is true overwhelmingly for the entire image, the four indicators of speckle reduction quality will remain almost the same. It will therefore be used as a stopping criterion. The flow-chart given in Figure 3 summarizes the proposed approach.

3.3 Simulation of speckled images

In order to create a speckled image from an original image we feed the SA-MS algorithm with the original image and set the temperature at a fix value; the algorithm is then run one time. The noise free image used in this work is the aerial photograph of a scene; it will be called *True-scene* [1]. Figures 4(b)-(f) show the results of the simulations with varying temperature T_0. It can be seen from Figure 4 that, as the temperature increases, so does the noise, resulting in a decreasing *SNR* as seen in Table I. For a temperature T_0 approaching zero, the Metropolis algorithm predicts no major change of the output compared to the current input; this is shown in Figure 4(b). Basically, in one hand if the temperature T_0 is set high, all configuration changes are accepted and only one scan of the image is enough to produce a very noisy image (see Figure 4(f)); on the other hand, if T_0 is set very low, almost no change is allowed and the output image is visually identical to its input (see Figures 4(a)-(b))

T_0	0	10	20	30	40	500
$SNR(\text{dB})$	27.84	14.34	11.12	9.92	9.27	7.06

Table I: Variation of the *SNR* in terms of T_0.

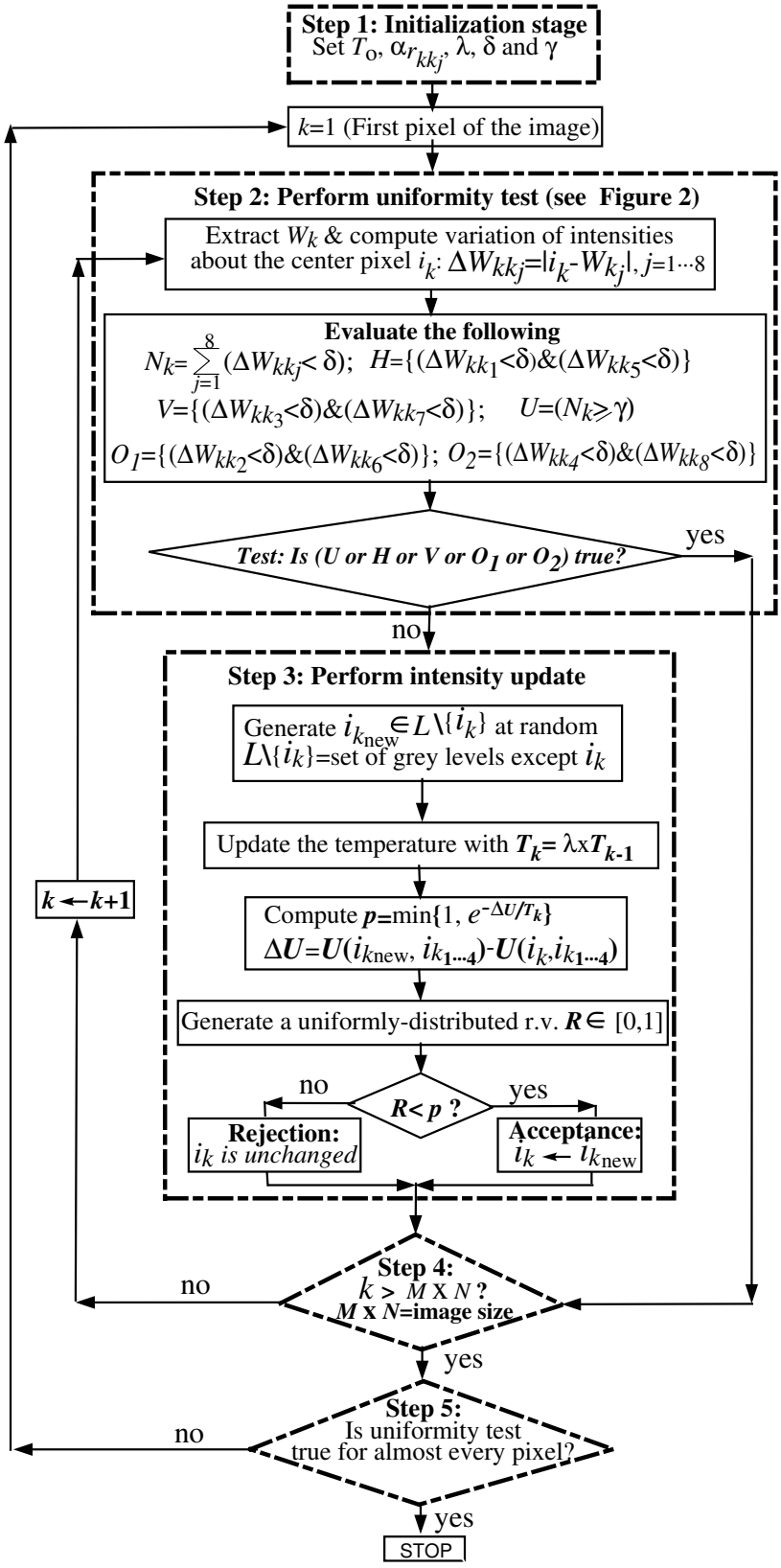

Figure 3: Flow-chart of the speckle reduction proposed approach.

(a)

(b)

(c)

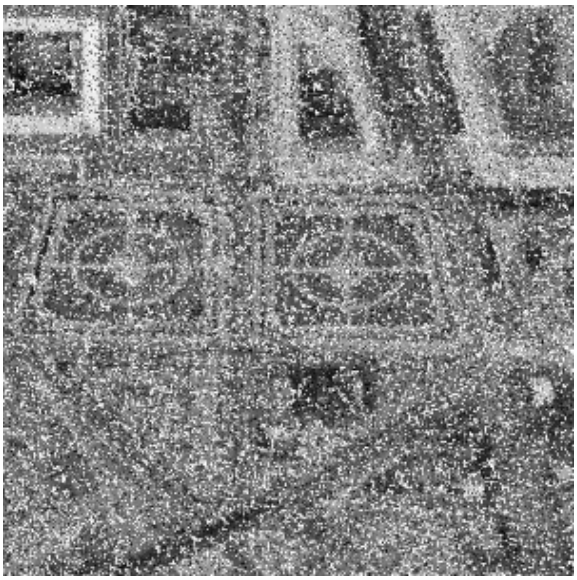

(d)

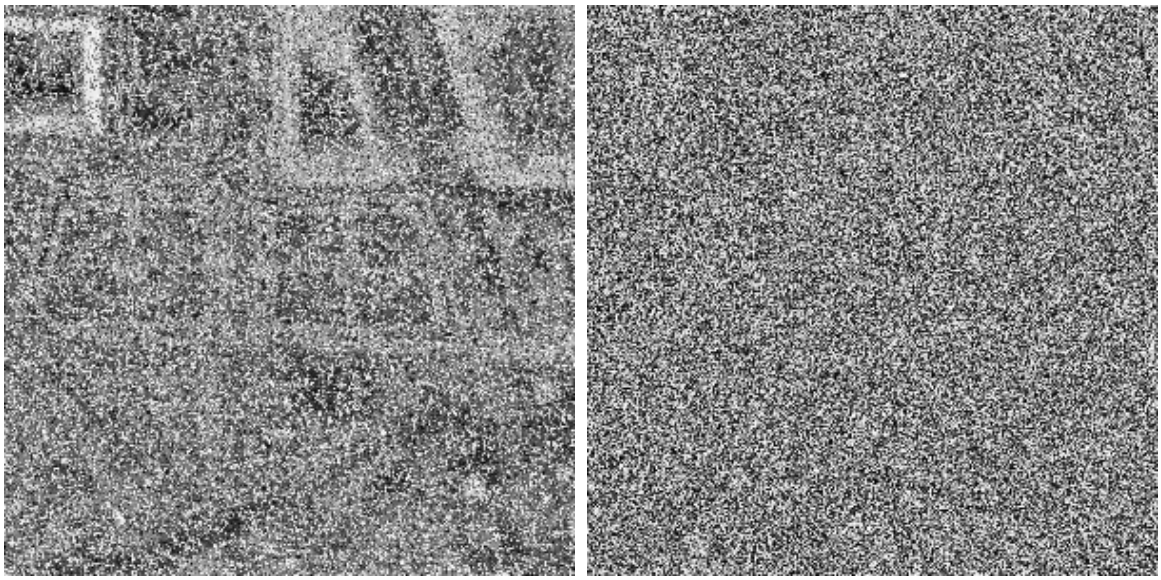

(e) **(f)**

Figure 4: (a) *True-scene*. (b) Speckled version of *True-scene* with $T_0 \to 0$ and SNR=27.84 dB. (c) Speckled version of *True-scene* with $T_0 = 10$ and SNR=14.34 dB. (d) Speckled version of *True-scene* with $T_0 = 20$ and SNR=11.12 dB. (e) Speckled version of *True-scene* with $T_0 = 40$ and SNR=9.92 dB. (f) Speckled version of *True-scene* with $T_0 = 500$ and SNR=7.06dB.

3.4 Speckle reduction of simulated speckled image

The goal here is to reduce the speckle existing in Figure 4(c). We compare our proposed approach against well-known speckle removal filters: the Gamma Map, the modified-Lee and the enhanced Frost filters [5]. The results of the speckle reduction are presented in Figure 5(c)-5(h). Table II gives a summary of the results. It is visually obvious that the proposed approach performs better: the results are not blurred and the features are better preserved. The metrics ENL, MSE, β, and SNR defined in Section 3.1 are evaluated for the proposed approach and compared to the other filters. From the figures shown and the results obtained, the proposed approach outperform the other filters. Besides, based on the stopping criterion described in Section 3.2, the proposed approach converge after the 82nd iteration (see Table II) since the values of the four metrics remain almost constant after the 82nd iteration.

	ENL	MSE	β	SNR(db)
Noisy image	21.96	760.02	0.3139	14.34
Gamma filtered	24.48	309.66	0.4427	18.24
Modified-Lee filtered	25.13	308.32	0.4289	18.26
Enhanced-Frost filtered	24.92	313.41	0.3808	18.19
Proposed approach after the 20th iteration	47.75	259.47	0.4606	19.01
Proposed approach after the 50th iteration	49.63	251.38	0.4652	19.15
Proposed approach after the 82nd iteration	49.73	251.15	0.4658	19.15
Proposed approach after the 100th iteration	49.73	251.18	0.4657	19.15

Table II: Results of speckle reduction using the simulated speckled image.

(a)

(b)

(c)

(d)

(e)

(f)

(g)

(h)

Figure 5: (a) *True-scene*. (b) Speckled version of *True-scene* with $T_0 = 10$ and SNR=14.34 dB. (c) Modified-Lee filtered version. (d) Gamma filtered version. (e) Enhanced-Frost filtered version. (f) Proposed approach after 20 iterations. (g) Proposed approach after 50 iterations. (h) Proposed approach after 82 iterations.

3.5 Application of speckle reduction to real SAR image

The SA-MS speckle reduction algorithm described in Section 3.2 is applied to a real SAR image [14]. Two sub-images of size 700×700 pixels have been extracted and used to test the proposed approach; they are shown in Figure 6. Let call these images Image-1 and Image-2, respectively. Note that the speckle reduction quality assessment of real SAR images are based on the ENL metric, since the other metrics required the knowledge of the true image, which does not exist for real SAR imagery.

Different speckle reduction filters, such as the Lee [12], the Frost [9], the Kuan [11], or the modified-Lee, the enhanced-Frost and the gamma MAP filters [5], have been tested and the best results were obtained with the enhanced-Frost. The results obtained for the modified-Lee the gamma Map and the enhanced-Frost are all presented in this report but the comparative analysis is only done between the enhanced-Frost and the proposed speckle reduction approach.

Figure 8(a) represents the noisy image Image-1 and Figure 8(b) is its filtered version using the enhanced-Frost; Figure 8(c)-(g) present its de-noised versions using the proposed approach after 14, 25, 50 and 80 iterations, respectively. The parameters of the MRF model are set on a case-by-case basis. For this image, the best results were obtained with $T_0 = 10^{-4}$, $\alpha_{r_{kk_j}} = 0.9$, $\lambda = 0.99$, $\delta = 5$, and $\gamma = 4$. Based on the ENL, after 14 iterations, the proposed approach performs better than the enhanced-Frost (see Table III). Besides, according to the stopping criterion discussed earlier, after the 80th iteration, the algorithm stops.

Let analyze and compare the image degradation due to the filtering process. Consider the bright "cross" in the middle of Image-1. This "cross" will be used to compare the resolution degradation between the proposed approach and the enhanced-Frost algorithm. At first glance, the"cross" seems to have a reduce resolution in the proposed approach (Figure 8(e)-(g)) compare to the enhanced-Frost (Figure 8(b)). Let us zoom around the shiny "cross". The results are shown in Figure 7. It is clear that the proposed approach let untouched the noise free area, here the bright "cross", and de-noises the rest, contrarily to the enhanced-Frost. As a consequence the proposed approach better preserve the edges compared to the enhanced-Frost approach.

	ENL
Image-1 (Noisy)	2.66
Gamma filtered version	7.64
Modified-Lee filtered version	7.96
Enhanced-Frost filtered version	8.08
Proposed approach after the 14th iteration	8.10
Proposed approach after the 25th iteration	9.93
Proposed approach after the 50th iteration	11.63
Proposed approach after the 80th iteration	12.21
Proposed approach after the 100th iteration	12.24

Table III: Speckle reduction using Image-1, (Note: The higher ENL is, the better is the speckle reduction.)

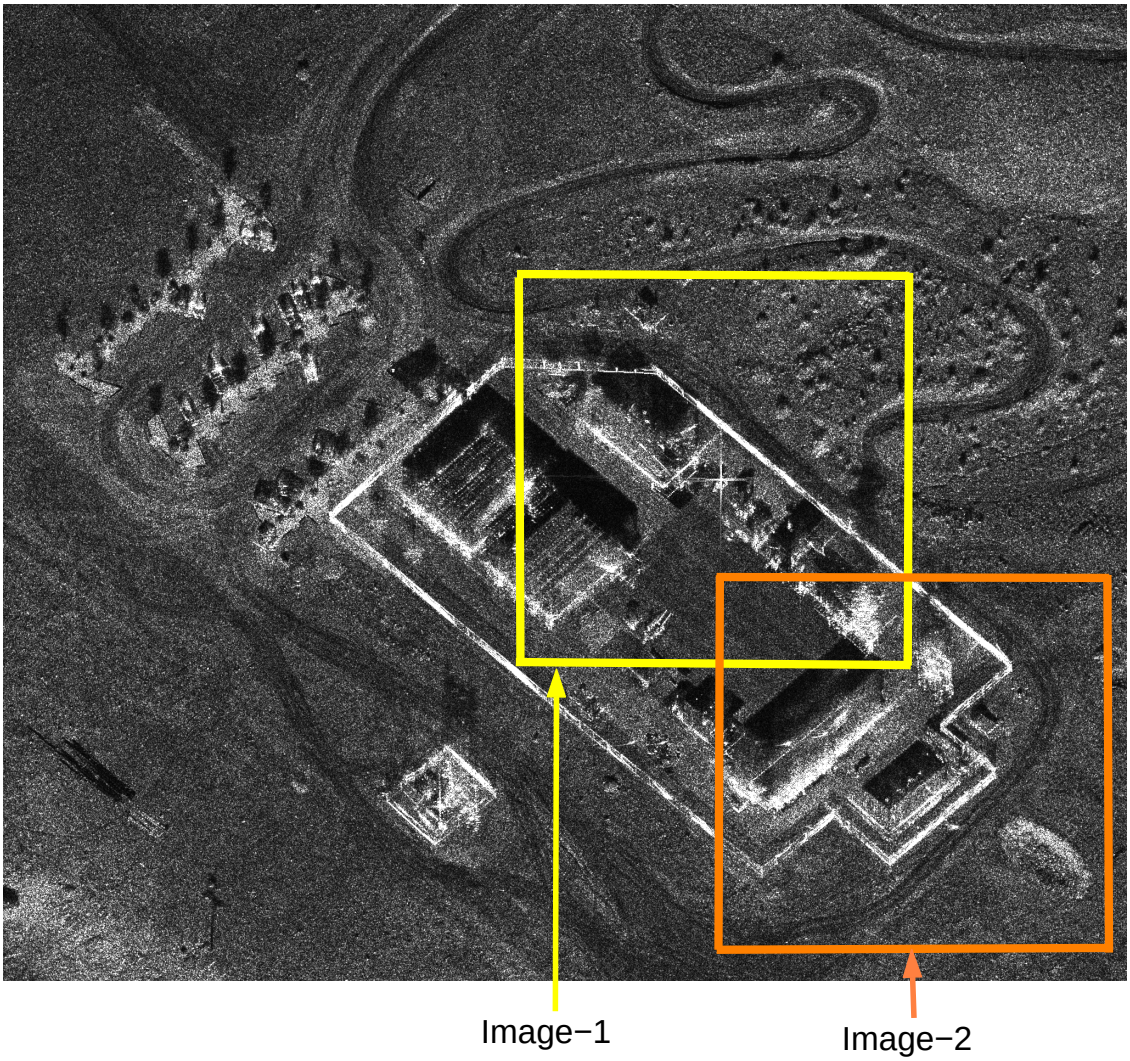

Figure 6: Full image showing the two extracted sub-images.

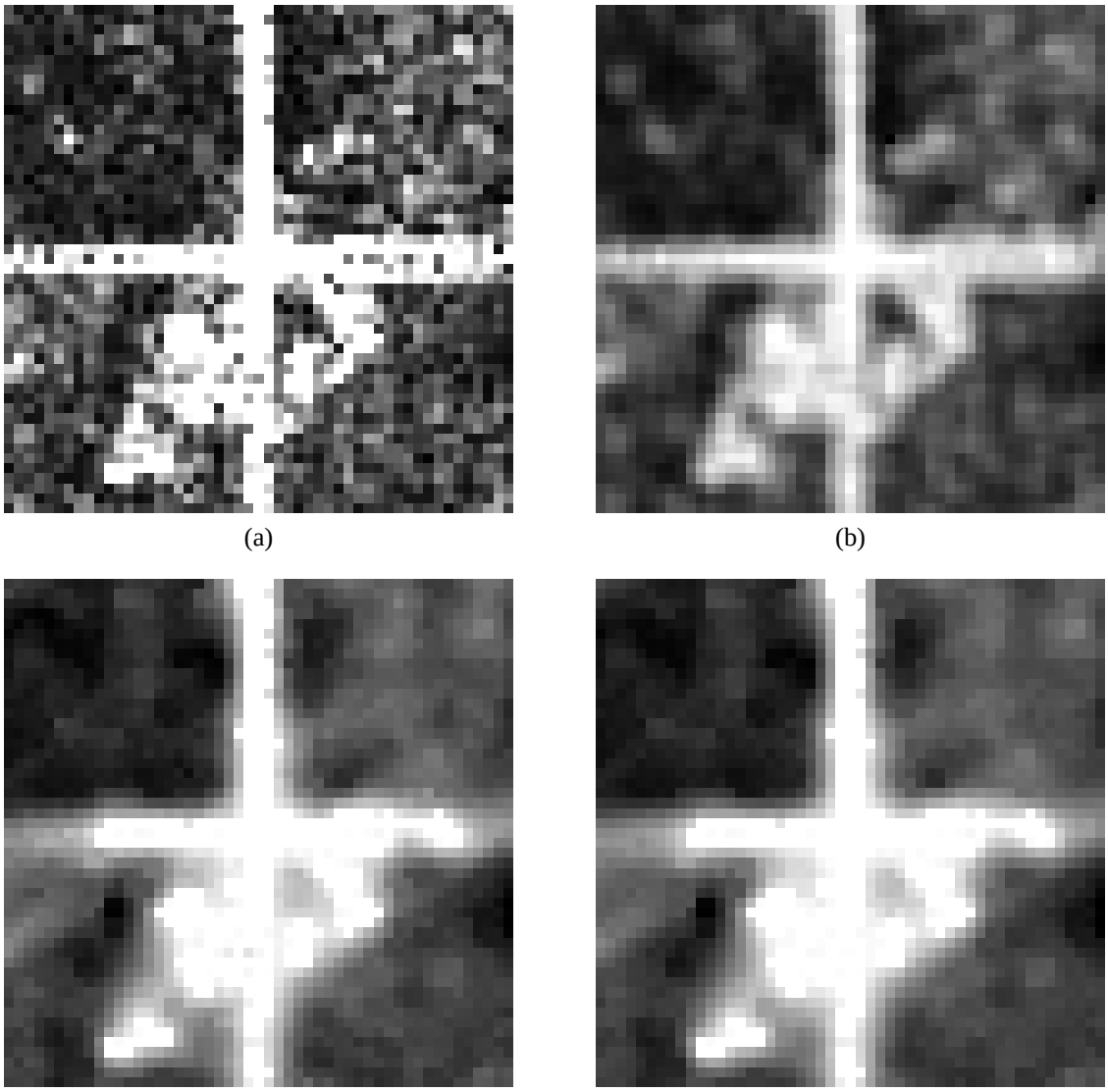

(a) (b)

(c) (d)

Figure 7: (a) First zoom on Image-1 (noisy). (b) First zoom on the enhanced-Frost filtered version of Image-1. (c) First zoom on the proposed speckle reduction approach of Image-1 after 50 iterations. (d) First zoom on the proposed speckle reduction approach of Image-1 after 80 iterations.

(a)

(b)

(c)

(d)

(e) (f)

(g) (h)

Figure 8: (a) Noisy Image-1. (b) enhanced-Frost. (c) Gamma-Map. (d) modified-Lee. (e) Proposed approach after 14 iterations. (f) Proposed approach after 25 iterations. (g) Proposed approach after 50 iterations. (h) Proposed approach after 80 iterations.

Let us zoom in another area of the image as seen on Figure 9. The result of speckle reduction are shown in Figure 10. Ones again, the proposed approach seems to be less blurred compared to the enhanced-Frost. A better illustration can be found in Figure 11. The impulse-like curve in blue represents the magnitude in dB of points from Figure 9 with same X-axis and whose Y-axis varies from index 295 to 310. The speckle reduction results after 25 and 50 iterations are compared with the enhanced-Frost. It can be seen from Figure 11 that the proposed approach has preserved the initial peak.

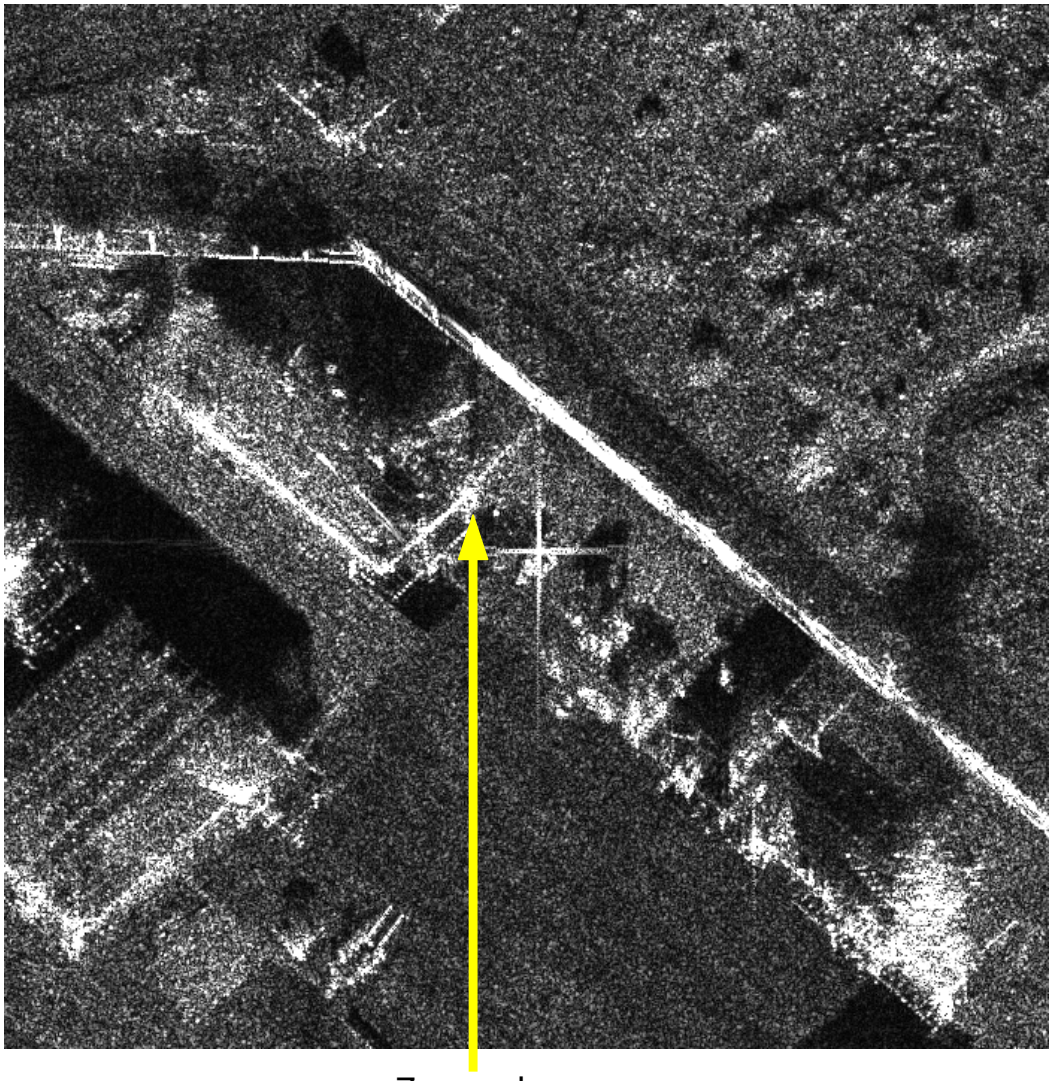

(a)

Figure 9: (a) Image-1 showing the second zoomed area.

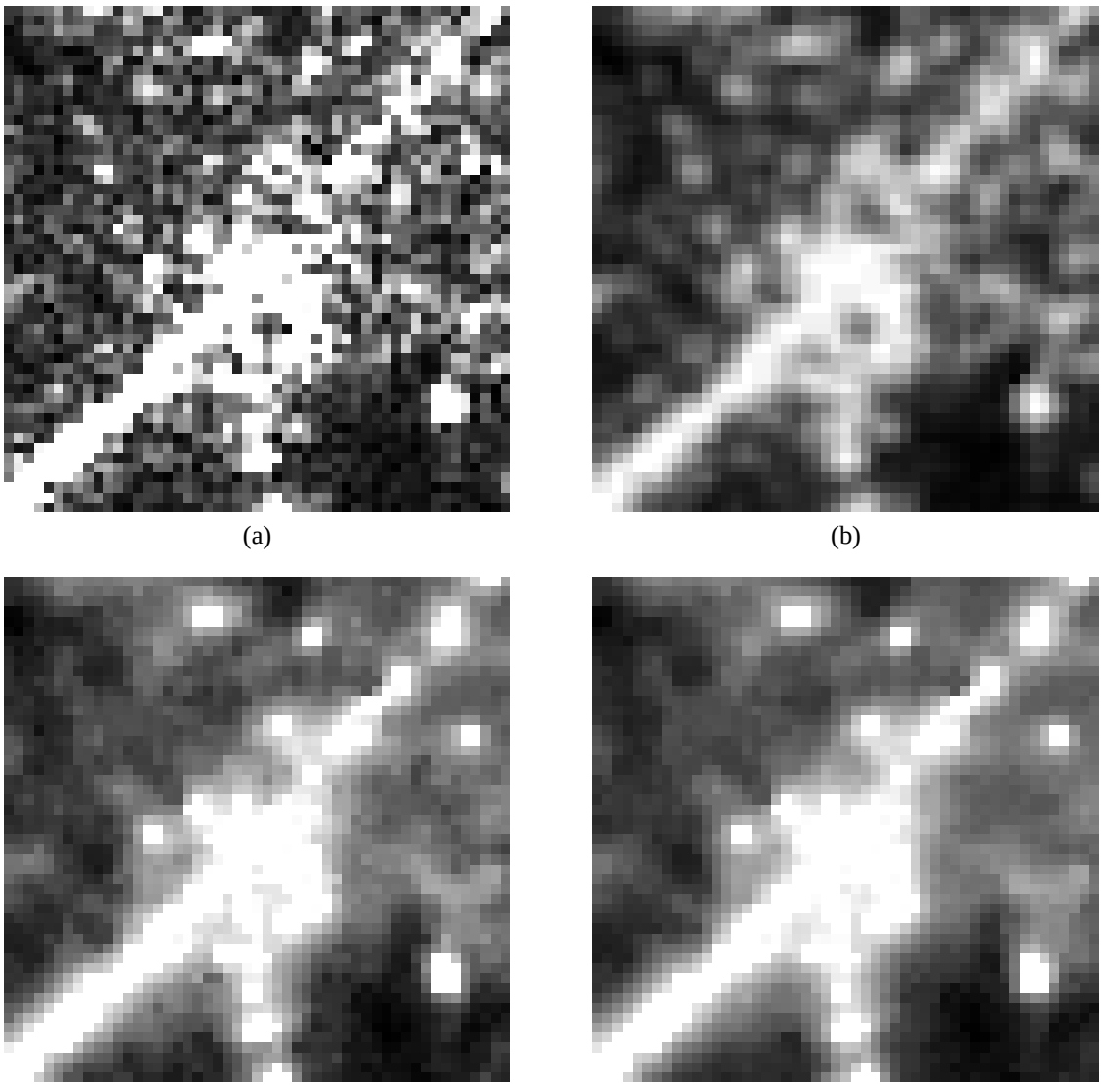

(a) (b)

(c) (d)

Figure 10: (a) Second zoom of Image-1(noisy). (b) Second zoom on the enhanced-Frost version of Image-1. (c) Second zoom on the proposed speckle reduction approach after 25 iterations. (d) Second zoom on the proposed speckle reduction approach after 50 iterations.

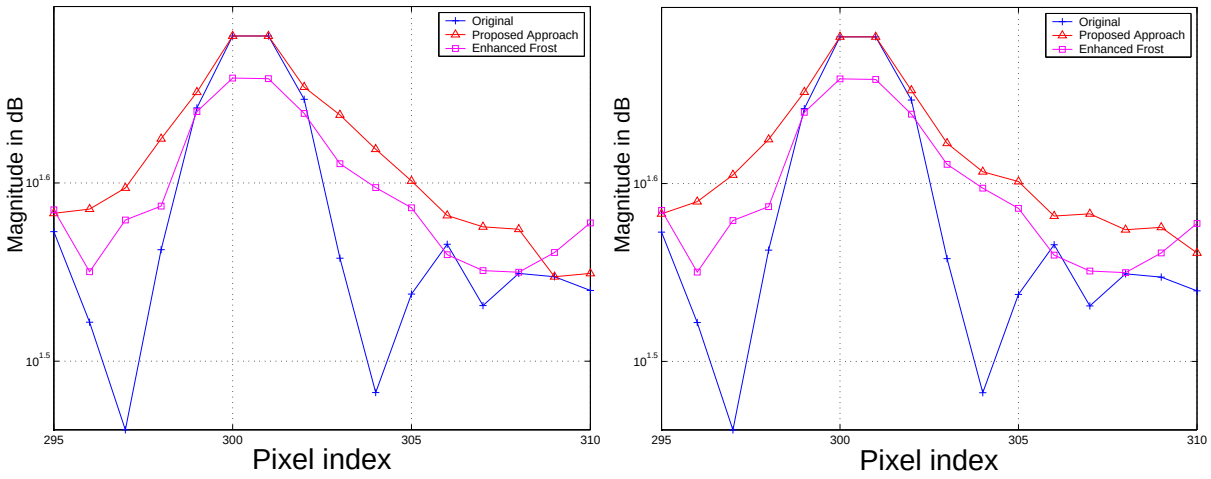

(a) (b)

Figure 11: (a) Original PSF-like curve, after enhanced-Frost and after 25 iterations of the proposed approach. (b) Original PSF-like curve, after enhanced-Frost and after 50 iterations of the proposed approach.

The second image (Image-2) is now processed. Figure 12 and Table IV give a summary of the results. For this image, the convergence occurs after 60 iterations. Then, an area of Image-2 shown in Figure 13 is zoomed, in order to compare the degradation effect on the edges due to the two speckle reduction approaches. The results are presented in Figure 14; once again, the results of the proposed approach seem to be less blurred compare to the enhanced-Frost.

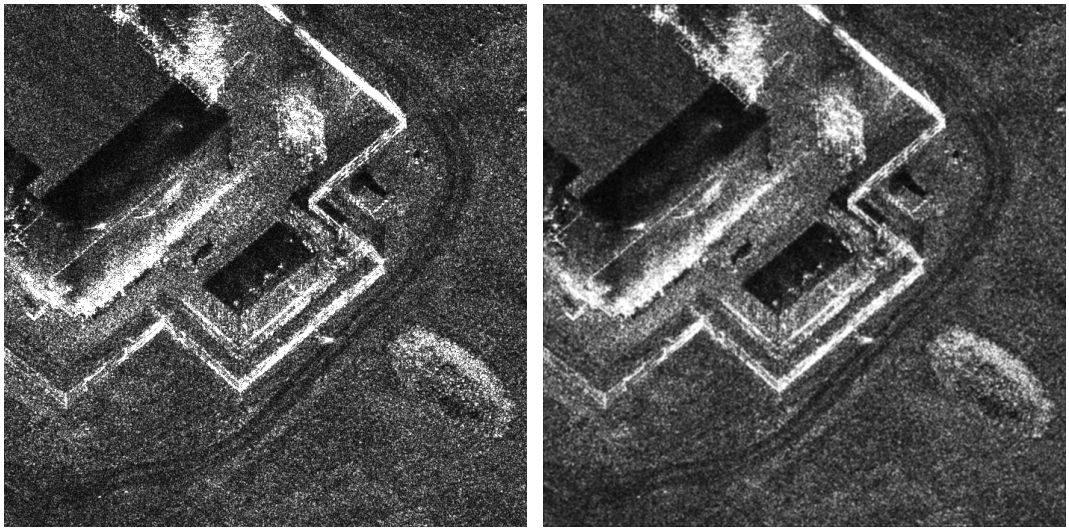

(a) (b)

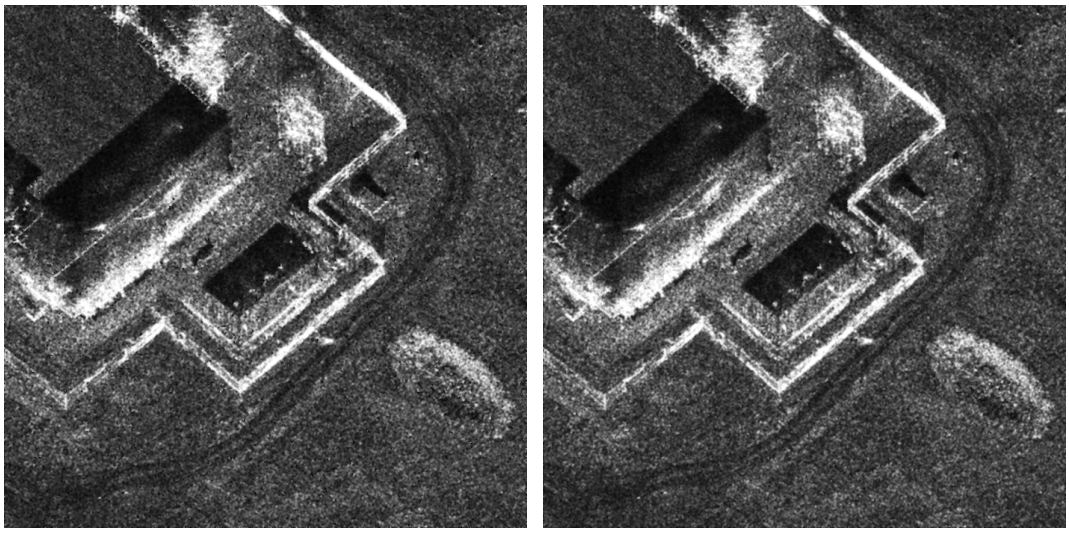

(c) (d)

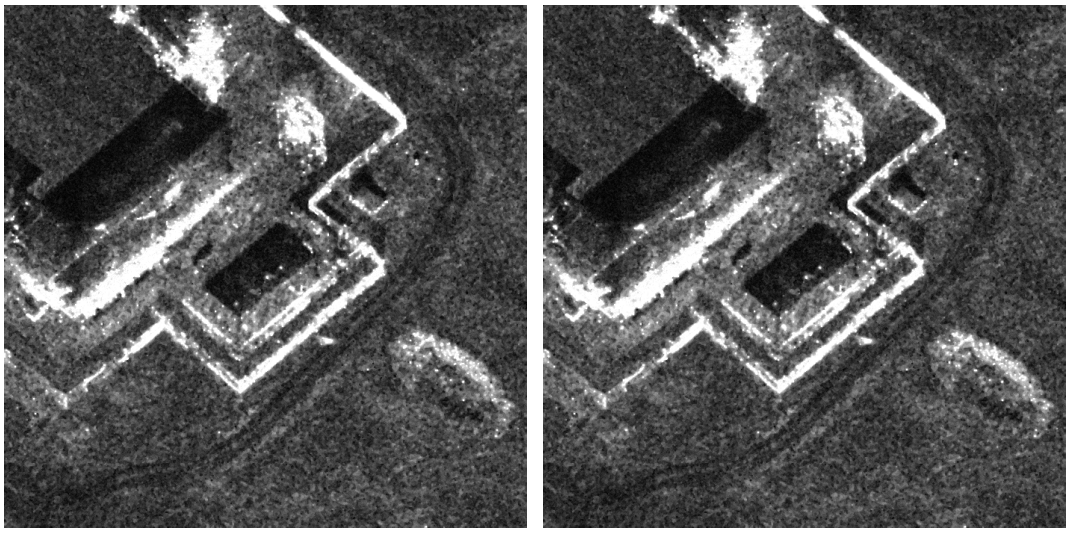

(e) (f)

Figure 12: (a) Noisy Image-2. (b) Enhanced-Frost. (c) Gamma-Map. (d) Modified-Lee. (e) Proposed approach after 46 iterations. (f) Proposed approach after 60 iterations.

	ENL
Image-2 (Noisy)	3.07
Gamma filtered version	9.39
Modified-Lee filtered version	10.17
Enhanced-Frost filtered version	10.39
Proposed approach after the 46th iteration	10.40
Proposed approach after 55th iteration	10.50
Proposed approach after 60th iteration	10.53
Proposed approach after 80th iteration	10.54

Table IV: Speckle reduction using Image-2 (Note: The higher ENL is, the better is the speckle reduction).

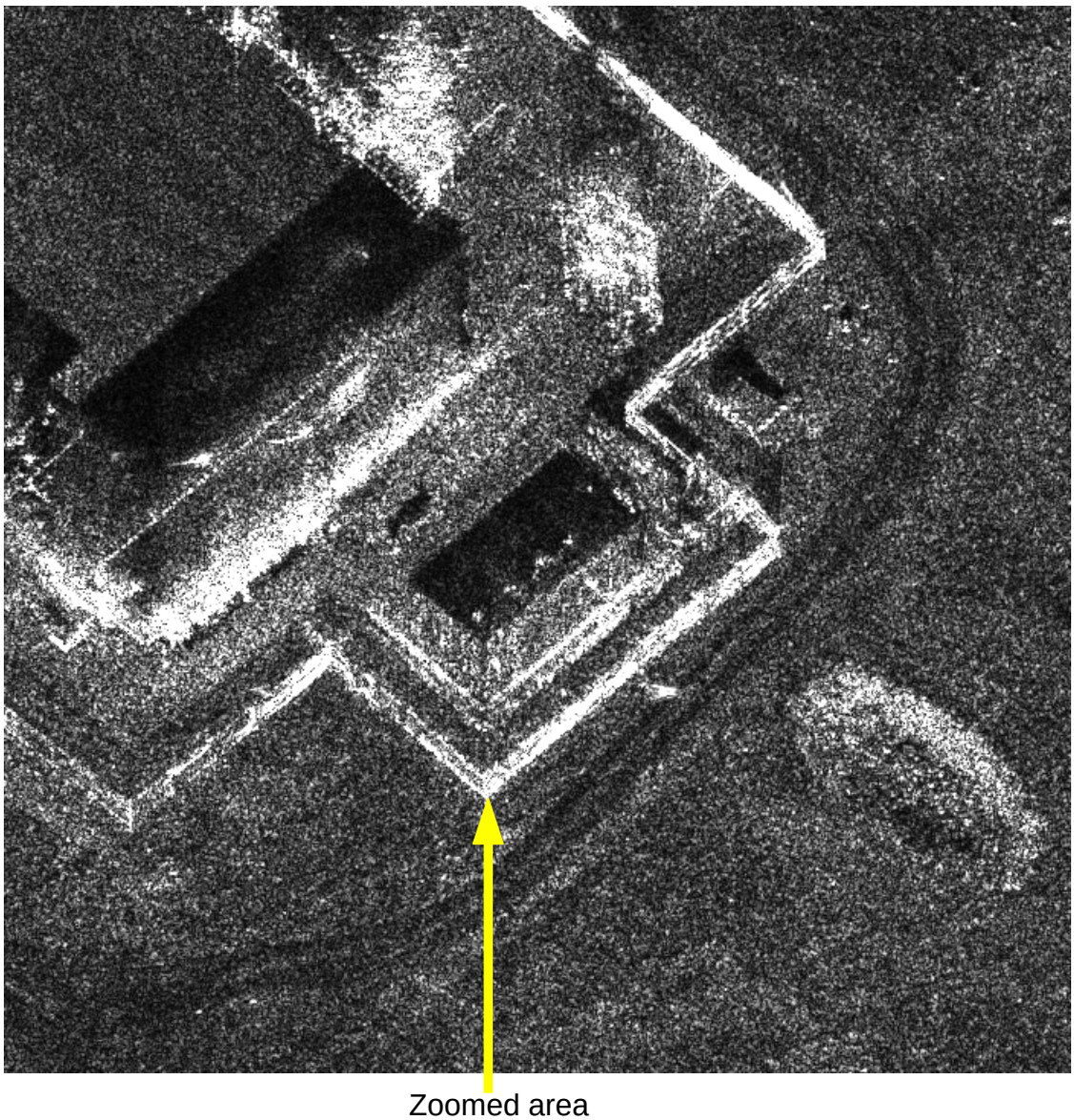

(a)

Figure 13: (a) Image-2 showing the zoomed area

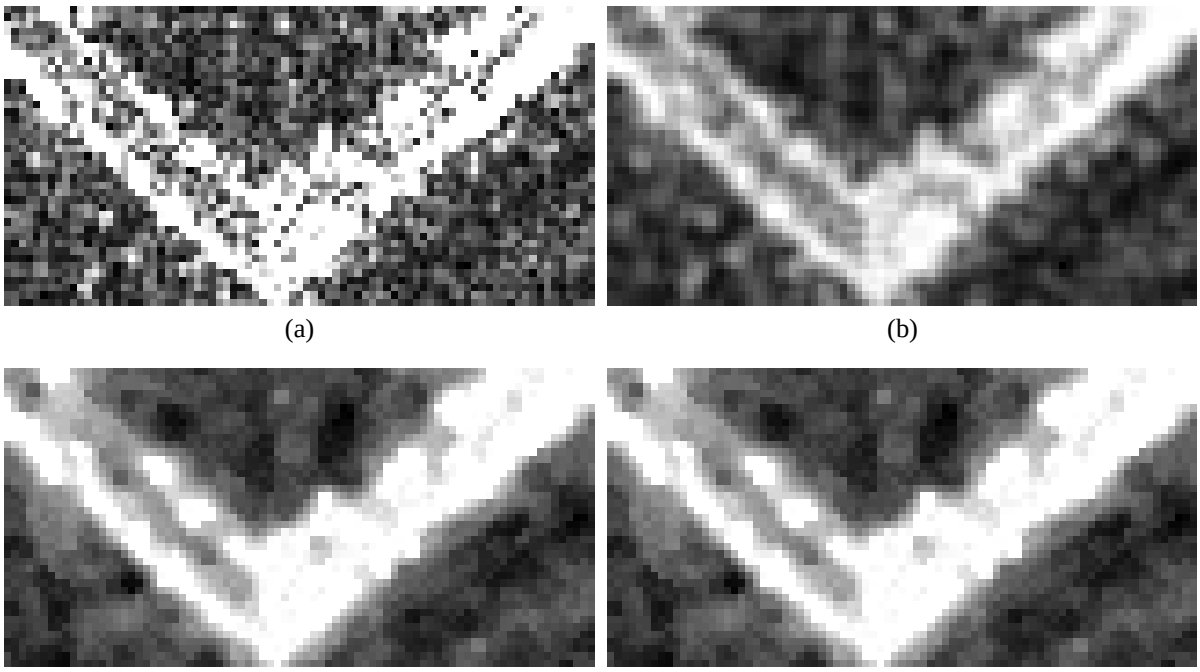

(a) (b)

(c) (d)

Figure 14: (a) Zoomed Image-2. (b) Zoomed enhanced-Frost. (c) Zoomed proposed approach after 46 iterations. (d) Zoomed proposed approach after 60 iterations.

4 Conclusion

The three major contributions of this report are: first, it presents a novel model of speckled imagery in the context of MRFs; second, the model is used together with the Metropolis SA algorithm to reduce the speckle in real SAR imagery; third, it introduces a stopping criterion for the SA in order to have an objective assessment of the convergence of the algorithm and avoid over-smoothed or blurred images.

The reduction process using our proposed approach seems to outperform the Gamma Map, the modified-Lee and the enhanced-Frost filters. Various speckled images have been tested showing a similar trend. Three main reasons can explain this improved performance. Firstly, the intrinsic spatially-correlated and signal-dependent nature of speckle noise makes the MRF framework a natural choice. Secondly, the SA, being an iterative method, allows a gradual and interactive noise removal compared to the standard methods [7]. Thirdly, since the energy function used in the SA is derived according to the physical model of the speckle, which, in turn, leads to a reliable speckle reduction.

Due to the computational complexity of the SA-MS algorithm, a more efficient version of the speckle denoising approach, within the same MRF framework, has also been developed showing comparable results. The new procedure is based on an optimal estimate of the true image intensity, in the sense of minimizing the MSE, and it is given by the conditional expectation of a pixel given its four neighbors. This alternate approach takes on Matlab approximately 5 minutes yielding $ENL = 8.23$ (using only one iteration!), compared to the SA-MS algorithm, which takes approximately 66 minutes to yield $ENL = 8.10$ (using 14 iterations).

The authors wish to thank Dr. Armin Doerry at Sandia National Laboratories for providing valuable suggestions and SAR imagery.

References

[1] http://vasc.ri.cmu.edu//idb/html/.

[2] Fabrizio Argenti and L. Alparone. Speckle removal from sar images in the undecimated wavelet domain. *IEEE Transactions on Geoscience and Remote Sensing*, 40(11):2363–2374, November 2002.

[3] J. Besag. Spatial interaction and the satatistical analysis of lattice systems. *J. R. Stat. Soc.*, Series B(36):192–236, 1974.

[4] J.C. Dainty. *Topic in Applied Physics: Laser Speckle and Related Phenomena*. Springer-Verlag, N.Y., 1984.

[5] A. Lopes *et al.* Adaptive Speckle Filters and Scene Heterogeneity. *IEEE Transactions on Geoscience and Remote Sensing*, 28(6):992–1000, Nov. 1990.

[6] Alin Achim *et al.* Sar image denoising via bayesian wavelet shrinkage based on heavy tailed modeling. *IEEE Trans. Geosci. Remote Sensing*, 41:1773–1784, 2003.

[7] Chris Oliver *et al. Understanding Synthetic Aperture Radar Images*. SciTech, NC 27613, 2004.

[8] G. Franceschetti *et al. Synthetic Aperture Radar Processing*. CRC Press, New York, 1999.

[9] V.S. Frost *et al.* A model for radar images and its application to adaptive digital filtering of multiplicative noise. *IEEE Trans. Pattern Anal. Machine Intell.*, 4(2):157–165, Mar. 1982.

[10] S. Kirkpatrick, C. Gelatt Jr., and M. Vecchi. Optimization by simulated annealing. Research report rc9355, IBM, 1982.

[11] D. T. Kuan, A. A. Sawchuk, T. C. Strand, and P. Chavel. Adaptive noise smoothing filter for images with signal-dependent noise. *IEEE Transactions. Pattern Anal. Machine Intell.*, PAMI(7):165–177, March 1985.

[12] Jong-Sen Lee. Speckle analysis and smoothing of synthetic aperture radar images. *CGIP*, 17(1):24–32, September 1981.

[13] N. Metropolis, A. Rosenbluth, M. Rosenbluth, A. Teller, and E. Teller. Equations of state calculations by fast computing machines. *The journal of Chemical Physics*, 21(6):1087–1092, 1953.

[14] Courtesy of Sandia National Laboratories.

[15] Thomas R. Crimmins. Geometric filter for reduction speckle. *Optical Engineering*, 25(5), May 1986.

[16] Ridha Touzi. A review of speckle filtering in the context of estimation theory. *IEEE Transactions on Geoscience and Remote Sensing*, 40(11):2392–2404, Nov. 2002.

[17] Hua Xie, L.E. Pierce, and F.T. Ulaby. Sar speckle reduction using wavelet denoising and markov random field modeling. *IEEE Transactions on Geoscience and Remote Sensing*, 40(10):2196–2212, October 2002.